Constraints on a general 3-generation neutrino mass matrix from neutrino data: application to the MSSM with R-parity violation

A. Abada [*], M. Losada [†]

Theory Division, CERN, CH-1211 Geneva 23, Switzerland

Abstract

We consider a general symmetric (3×3) mass matrix for three generations of neutrinos. Imposing the constraints, from the atmospheric neutrino and solar neutrino anomalies as well as from the CHOOZ experiment, on the mass squared differences and on the mixing angles, we identify the ranges of allowed inputs for the 6 matrix elements. We apply our results to Majorana left-handed neutrino masses generated at tree level and through fermion–sfermion loop diagrams in the MSSM with R-parity violation. The present experimental results on neutrinos from laboratories, cosmology and astrophysics are implemented to either put bounds on trilinear $(\lambda_{ijk}, \lambda'_{ijk})$ and bilinear $(\mu_{e,\mu,\tau})$ R-parity-violating couplings or constrain combinations of products of these couplings.

Pacs numbers: 13.15.+g, 14.70.Bh, 95.30.Cq.

Typeset using REVTEX

[*]e-mail: abada@mail.cern.ch. On leave of absence from the Laboratoire de Physique Théorique, bât 210, Université de Paris XI, 91405 Orsay, France.

[†]e-mail: losada@mail.cern.ch. On leave of absence from the Universidad Antonio Nariño, Santa Fe de Bogotá, Colombia.

arXiv:hep-ph/9908352v2 12 Oct 2000

I. INTRODUCTION

The current experimental evidence strongly suggests the existence of a non-trivial structure of the mass matrix for 3 generations of neutrinos. Indeed, deficits of the solar electron neutrino and atmospheric muon neutrino fluxes compared to their theoretical predictions are strong evidence in favour of neutrino oscillations as an explanation of these deficits. Furthermore, oscillations of neutrinos imply masses for neutrinos and mixing angles, which relate the flavour basis to the mass eigenstate basis, as is the case in the quark sector.

Observations in favour of the oscillation solutions came recently with the Super-Kamiokande collaboration [1] results, which have to be added to those of other atmospheric neutrino experiments (IMB [2], Soudan [3], Kamiokande [4]) and solar neutrino experiments (Homestake [5], Gallex [6], SAGE [7], Kamiokande [8], Super-Kamiokande [9], MACRO [10] and LSND [11]). The oscillation explanation [1] of the solar neutrino problem, the atmospheric neutrino anomaly and the LSND results suggest three very different values of neutrino mass squared differences, namely $\Delta m^2_{\text{sun}} \ll \Delta m^2_{\text{atm}} \ll \Delta m^2_{\text{LSND}}$, with $\Delta m^2_{\text{sun}} \lesssim 10^{-4}$ eV^2, $\Delta m^2_{\text{atm}} \in [10^{-3}, 10^{-2}]$ eV^2 and $\Delta m^2_{\text{LSND}} \in [0.3, 10]$ eV^2. The evidence for $\bar{\nu}_\mu \to \bar{\nu}_e$ observed by LSND has not been confirmed or excluded by the KARMEN [16] experiment. The MiniBooNE at FNAL or MINOS long-baseline experiments could provide the answer. Given the atmospheric and solar neutrino observations, and excluding the LSND results [2], the deduced pattern of neutrino masses and mixing requires two different neutrino mass squared differences and three mixing angles. Recent interest in this subject has produced a very large number of possible models, which can accommodate the data, see refs. [17] for more details.

Our approach differs from most of the analyses in that we do not specify the model initially. In a general manner, we will use the current relevant information on the mixing angles and mass squared differences to constrain the neutrino mass matrix elements in the flavour basis $(\nu_e, \nu_\mu, \nu_\tau)$. Consequently this will constrain the parameters of the involved model. The results of this work can be applied to any class of model with three neutrino

---

[1]Other possible solutions, which could accommodate the experimental neutrino data, can involve flavour-violating interactions, or other more exotic possibilities such as the violation of Lorentz invariance [12] or the equivalence principle [13]. However, in the case of atmospheric neutrinos, it has been shown [14], [15] that neutrino decays or modification of special or general relativity do not fit the data.

[2]In a forthcoming analysis, we will include LSND results, which calls for a fourth neutrino species or a sterile neutrino.

generations. We also present an application of our results of the specific Minimal Supersymmetric Standard Model (MSSM) with R-parity violation. We will also try to elucidate if any of the different possible neutrino spectra (degenerate neutrinos, hierarchical, pseudo-Dirac [18]) are preferred for each solution of the solar anomaly combined with SuperKamiokande and CHOOZ constraints. Even barring the presence of a sterile neutrino, other interesting bounds on neutrino masses arise from cosmological or astrophysical sources, such as having a neutrino component of hot dark matter (HDM). In addition, low energy experiments can also constrain neutrino masses; the strongest constraint, which is applicable when the neutrinos are Majorana particles, arises from neutrinoless double beta decay. We will also analyse our results in view of the two latter bounds.

The neutrino is massless in the Standard Model and, if massive, requires the presence of new physics. For reviews, concerning models for neutrino masses and neutrino properties, see [19–22] and references therein. If the neutrino has a Majorana mass, the model must violate lepton number conservation. In supersymmetric (SUSY) extensions, gauge invariance and renormalizability no longer ensure lepton number L (or baryon number B) conservation. The generalization of the MSSM, which allows R-parity (R_P) violation ($R_P = (-1)^{L+3B+2S}$, where L, B, S are the lepton and baryon number and the spin of the particle, respectively), allows left-handed neutrinos to obtain a Majorana mass, at tree level through mixing with the neutralinos, and through loop diagrams that violate lepton number (in two units). We apply our general results to the MSSM with R-parity violation at one-loop order, allowing the presence of both bilinear and trilinear R_P-violating couplings without imposing any hierarchy between the parameters. We thus constrain all relevant R_P-conserving and non-conserving couplings by imposing the constraints from atmospheric and solar neutrino anomalies and the CHOOZ experiment. As a by-product, we see that in this model the constraints from neutrinoless double beta decay and cosmology are *automatically* satisfied.

The paper is organized as follows. In section II we expand on the inputs used. In section III we establish our notation for the general case of a 3-generation neutrino mass matrix. In section IV we introduce our notation for an application of our general results to the MSSM with R_P-violation. We also give the results for the tree-level neutrino mass matrix and the loop corrections to each matrix element. We start by parametrizing the general neutrino eigenmasses and eigenstates and use the neutrino data to constrain the ranges of variation of the general inputs. In section IV.A we introduce a toy-model that corresponds to several limiting cases of the MSSM without R-parity conservation. In section V we present our results for the general case and for the specific case of Majorana masses arising in the R-parity violating model. Finally in section VI we summarize and conclude.

II. GENERAL INPUTS

In this work, we compute the masses and mixing angles of the neutrino spectrum assuming three generations of neutrinos (this means that we are not taking the LSND result into account). We then apply all relevant existing bounds on the neutrino masses and mixing angles to constrain the elements of our neutrino mass matrix in the flavour basis. These inputs are from laboratories such as the CHOOZ experiment [23], the relevant mass squared differences Δm^2 and mixing angles $\sin^2 2\theta$ assuming the oscillation solution as an explanation of the solar and atmospheric neutrino deficits. We then check whether the upper bound coming from neutrinoless beta decay $(\beta\beta)_{0\nu}$ [24–26] and also the global cosmological upper bound on the sum of the neutrino masses [27] are satisfied. The best limit on the effective mass m_{eff} appearing in $(\beta\beta)_{0\nu}$, and defined by

$$|m_{\text{eff}}| = |\sum_i m_{\nu_i} U_{ei}^2| \leq \sum_k m_{\nu_k} |U_{ek}^2|, \tag{1}$$

has been derived in the Heidelberg–Moscow ^{76}Ge experiment [24]: $|m_{\text{eff}}| < (0.5 - 1.0)$ eV (at 90% C.L.). The CP phases that might appear in the mixing matrix U_{ek} are not relevant in our derivation, because we only use the second r.h.s. term in eq. (1). Another direct upper bound comes from the measurement of the high energy part of the ^{3}H β-decay spectrum: the upper limits on the electron neutrino mass obtained in the TROITSK [28] and MAINZ [29] experiments are $m_\nu < 2.5$ eV and $m_\nu < 3.4$ eV, respectively. However, these experiments suffer from some ambiguities referred to as "the negative mass squared problem", which is still not completely understood and we will therefore not use their bounds.

There are also upper bounds on the neutrino masses coming from astrophysical and cosmological considerations such as the one from hot dark matter (HDM), which suggests that $\sum_i m_{\nu_i} = m_1 + m_2 + m_3 < $ few eV [3].

Global fits to the data show that neutrino oscillations among three neutrino flavours are sufficient to accommodate the solar and atmospheric data [18], [31], [32], [33], [34]. Three different types of solar experiments (using different detectors: chlorine, gallium and Cherenkov) are sensitive to different solar neutrino energy ranges; to accommodate them, three regions of oscillation parameter space are allowed [31], [34], [35], which correspond to the vacuum oscillation solution, MSW with a large mixing angle (MSW-LMA) and MSW

---

[3]A recent analysis (observation of distant objects favouring a large cosmological constant instead of HDM) suggesting a non-zero cosmological constant [30] shows that the bound of a few eV for the sum of the neutrino masses is no longer imposed, since a hot dark matter component is not a necessary ingredient in this case.

with a small mixing angle (MSW-SMA). The estimates required to fit the data for the neutrino mass squared differences and the mixing angles are shown in table I. It is important to keep in mind that the neutrino oscillation scenario can only restrict mass squared differences but not fix the absolute neutrino mass scale; moreover, it cannot distinguish whether the smallest mass splitting, which corresponds to the solar data, is between the two lightest mass eigenstates or the two heavier ones.

To fix our notation, for this case with three generations, the flavour states ν_l are expressed in terms of the mass eigenstates ν_i using the 3×3 mixing matrix U

$$\nu_\ell = \sum_{i=1}^{3} U_{\ell i}^* \nu_i. \tag{2}$$

We hierarchically order the mass eigenvalues and denote them m_i, $i = 1, 2, 3$, such that

$$m_1 \leq m_2 \leq m_3.$$

In view of the ranges of the mass squared in table I, if the neutrino spectrum is hierarchical, then $\Delta m_{12}^2 = m_2^2 - m_1^2$ is the parameter relevant to the solar case and $\Delta m_{13}^2 = m_3^2 - m_1^2$ is the dominant one for the atmospheric case with $\Delta m_{12}^2 \ll \Delta m_{13}^2$ and $\Delta m_{23}^2 \sim \Delta m_{13}^2$. The corresponding mixing angles (see the parametrization below) are $\sin^2 2\theta_{12}$ and $\sin^2 2\theta_{23}$, respectively. Besides the hierarchical mass spectrum, there exist two other alternative neutrino spectra [18], [36], one in which the three neutrinos are quasi-degenerate and another (called pseudo-Dirac) in which only two neutrinos are quasi-degenerate and the third is much lighter (or heavier). In table II we show the different possible regimes and indicate which is the corresponding mass squared difference.

Experiment	Δm^2 (eV^2)	$\sin^2 2\theta$
Atmospheric	$(1 - 8) \times 10^{-3}$	$0.85 - 1$
Solar		
–MSW-LMA	$(3 - 30) \times 10^{-5}$	$0.6 - 1$
–MSW-SMA	$(0.4 - 1) \times 10^{-5}$	$10^{-3} - 10^{-2}$
–Vacuum	$(0.5 - 8) \times 10^{-10}$	$0.5 - 1$
CHOOZ	$> 3 \times 10^{-3}$	$\sin \theta_{13} < 0.22$

TABLE I. MSW-LMA, MSW-SMA and Vacuum stand for MSW large mixing angle, small mixing and vacuum oscillation solutions, respectively.

III. COMPUTATION OF THE MASS AND MIXING MATRIX

Spectrum	Solar	Atmospheric
Hierarchy	Δm_{12}^2	Δm_{13}^2
Degenerate	Δm_{23}^2 or Δm_{12}^2	Δm_{13}^2
Pseudo-Dirac	Δm_{23}^2 or Δm_{12}^2	Δm_{13}^2

TABLE II. Different possible regimes and corresponding mass squared difference.

A. Generic mass matrix

We consider a general 3×3 symmetric mass matrix in the flavour basis for three generations of neutrinos $(\nu_e, \nu_\mu, \nu_\tau)$:

$$\mathcal{M} = \begin{pmatrix} M_{11} & M_{12} & M_{13} \\ M_{12} & M_{22} & M_{23} \\ M_{13} & M_{23} & M_{33} \end{pmatrix} . \tag{3}$$

We construct the mass squared differences of the eigenvalues of $\mathcal{M}$ and the mixing matrix, which relates the flavour basis to the mass eigenstates, in a general way in terms of these input elements. We denote the three mass eigenvalues by m_i for $i = 1, 2, 3$, which satisfies, as mentioned above, the hierarchy $m_1 \leq m_2 \leq m_3$. For any given model, these masses and also the mixing matrix would be given in terms of the parameters of the model. We then apply the constraints, given in table I, individually and combined. The combined constraints are obtained by requiring the atmospheric, CHOOZ and one of the solar solutions to be satisfied simultaneously. In this way we can determine the region, in the $(\Delta m^2, \sin^2 2\theta)$ plane, that satisfies each of the three possible combinations of constraints simultaneously. The answer is then translated into terms of ranges where the parameters of the model vary so as to fulfil neutrino data constraints.

B. Generic mixing matrix

Computing the mass eigenstates of the mass matrix (3), we obtain the rotation matrix, which contains the relevant mixing angles. We use the Chau and Keung parametrization of a 3×3 matrix [37] given by

$$U = \begin{pmatrix} c_{12} \, c_{13} & s_{12} \, c_{13} & s_{13} e^{-i\delta} \\ -s_{12} \, c_{23} - c_{12} \, s_{23} \, s_{13} e^{i\delta} & c_{12} \, c_{23} - s_{12} \, s_{23} \, s_{13} e^{i\delta} & s_{23} \, c_{13} \\ s_{12} \, s_{23} - c_{12} \, c_{23} \, s_{13} e^{i\delta} & -c_{12} \, s_{23} - s_{12} \, c_{23} \, s_{13} e^{i\delta} & c_{23} \, c_{13} \end{pmatrix} \text{diag}\left\{ e^{i\alpha_1}, e^{i\alpha_2}, 1 \right\}, \quad (4)$$

where $c_{ij} = \cos(\theta_{ij})$ and $s_{ij} = \sin(\theta_{ij})$, δ is the Dirac CP phase and $\alpha_{1,2}$ are the Majorana ones (we have two additional CP phases in the case of Majorana particles). As previously

mentioned, we are going to work with a real mixing matrix and will ignore CP phases because we are interested in our derivation in the modulus of the matrix elements, as we will see.

The survival probability $P_{\nu_e \to \nu_e}$, relevant to the case of solar fluxes, depends only on the first row of the mixing matrix in eq. (4), i.e. on $|U_{ei}|^2$, with $i = 1, 2, 3$. In the atmospheric case, the oscillation probability depends on the last column of (4), i.e. on $|U_{\ell 3}|^2$, with $\ell = e, \mu, \tau$. The other elements of the matrix are not constrained by any direct experimental observation. With this parametrization, we directly obtain the parameters $\sin^2 2\theta_{12}$ and $\sin^2 2\theta_{23}$ and also the relevant CHOOZ parameter $\sin \theta_{13}$, which we need for our general analysis.

IV. APPLICATION: MSSM WITH R-PARITY VIOLATION

The specific R_P-violating model to which we apply our general results has been extensively analysed in the context of pure phenomenology, as well as in trying to fit the data of neutrino anomalies. In refs. [18] [38], [39], [40], [41], [42], [43], [44], [45], [46], [47] different phenomenological aspects of this theory have been analysed with respect to neutrino masses. In particular, refs. [40,41] have established in a basis-invariant way that neutrino masses are always generated in these models even when universality of the soft SUSY-breaking terms is assumed at some high scale. Previous studies have also tried to constrain the different R_P-violating couplings that appear in the MSSM Lagrangian, considering only the effect of bilinear terms [48]– [51] or only of trilinear couplings [52]– [54], or from both [56]– [60], solar and atmospheric neutrino data. Both tree-level and one-loop effects have been considered.

As stated in the introduction here we do not bias our selection of R_P-violating couplings, which would be contrary to a common practice of keeping only one R-parity-violating parameter at a time. We also include all possible bilinear and trilinear parameters for the MSSM without R-parity. In addition we do not impose any hierarchy between the trilinear couplings. Finally, our results present the allowed ranges for these parameters using the solar and atmospheric anomalies and the result from the CHOOZ experiment only. We will present our comparison to previous analyses in the last section.

The most general renormalizable superpotential for the supersymmetric Standard Model with lepton-number violation is

$$W = \epsilon_{ab}[\mu_\alpha \hat{L}_\alpha^a \hat{H}_u^b + \lambda_{\alpha\beta k} L_\alpha^a \hat{L}_\beta^b \hat{E}_k^C + h_{ik}^u \hat{Q}_i^a \hat{H}_u^b \hat{U}_k^C + \lambda'_{\alpha ik} \hat{L}_\alpha^b \hat{Q}_i^a \hat{D}_k^C], \qquad (5)$$

the (i, j, k) are flavour indices, (a, b) are $SU(2)$ indices, and the (α, β) are flavour indices running from 0 to 3. The $\hat{L}_\alpha$ are the doublet superfields with hypercharge $Y = -1$. Note that the λ couplings are antisymmetric in the first two indices. The usual R-parity-preserving Lagrangian is obtained when only $\mu_o, \lambda_{0ik} = h_{ik}^d, \lambda'_{i0k} = h_{ik}^d$ are non-zero and we can identify

$\hat{L}_o \equiv \hat{H}_d$. In the model of eq. (5) we have 9 additional λ couplings and 27 new λ' couplings compared to the R-parity-conserving case. Note that thanks to the additional degrees of freedom, we can rotate in the flavour space of the "down-type" scalar fields to set the vacuum expectation values of the sleptons to be zero [4]. Henceforth, we will work consistently in this basis.

We use the following parametrization for the tree-level mass matrix in the basis of charged-lepton eigenstates:

$$
\mathcal{M}_\nu^{tree} = \begin{pmatrix} \alpha_e^2 & \alpha_\mu \alpha_e & \alpha_e \alpha_\tau \\ \alpha_\mu \alpha_e & \alpha_\mu^2 & \alpha_\mu \alpha_\tau \\ \alpha_e \alpha_\tau & \alpha_\mu \alpha_\tau & \alpha_\tau^2 \end{pmatrix} ; \tag{6}
$$

the corresponding expressions for the α_i's are given in appendix B. This tree-level mass matrix has only **one** non-zero eigenvalue. It is thus necessary to include additional corrections, which could provide two different mass splittings.

The loop corrections, shown in fig. 1, from slepton–lepton and squark–quark loops to each element of the mass matrix are given by [39],

$$
(m_{qm})_{\text{loop}} = \frac{1}{16\pi^2} \left(\sum_{k,p} \lambda_{qkp} \lambda_{mpk} m_\ell^{(k)} \sin 2\phi_\ell^{(p)} \ln \frac{M_1^{(p)}}{M_2^{(p)}} + 3 \sum_{k,p} \lambda'_{qkp} \lambda'_{mpk} m_q^{(k)} \sin 2\phi_q^{(p)} \ln \frac{M_{q1}^{(p)}}{M_{q2}^{(p)}} \right). \tag{7}
$$

Here the angles $\phi_\ell^{(p)}$ and $\phi_q^{(p)}$ are given in terms of the slepton and squark mass eigenstates for a given flavour (p) $M_{1,2}$ and $M_{q1,q2}$ as

$$
\sin 2\phi_\ell^{(p)} \ln \frac{M_1^{(p)}}{M_2^{(p)}} = m_\ell^{(p)} \left(\frac{2X}{M_1^{(p)\,2} - M_2^{(p)\,2}} Ln \left(\frac{M_1^{(p)}}{M_2^{(p)}} \right) \right) = m_\ell^{(p)} \left(\frac{X}{M_2^{(p)\,2}} f(x_\ell^{(p)}) \right) \tag{8}
$$

$$
\sin 2\phi_q^{(p)} \ln \frac{M_{q1}^{(p)}}{M_{q2}^{(p)}} = m_q^{(p)} \left(\frac{2X}{M_{q1}^{(p)\,2} - M_{q2}^{(p)\,2}} Ln \left(\frac{M_{q1}^{(p)}}{M_{q2}^{(p)}} \right) \right) = m_q^{(p)} \left(\frac{X}{M_{q2}^{(p)\,2}} f(x_q^{(p)}) \right), \tag{9}
$$

where $m_{\ell,q}^{(p)}$ are lepton and quark masses of flavour p; $X = A + \mu \tan \beta$ [61], which we take to be universal, and provides a mixing term between the left- and right-handed squarks and sleptons. The function f is defined to be

$$
f(x) = -\frac{\ln x}{1-x}, \quad x_\ell^{(p)} = \left(\frac{M_1^{(p)}}{M_2^{(p)}} \right)^2 \quad \text{and} \quad x_q^{(p)} = \left(\frac{M_{q1}^{(p)}}{M_{q2}^{(p)}} \right)^2. \tag{10}
$$

---

[4]This can be done order by order in the loop expansion when one appropriately defines the mass matrices of the Higgs sector [58].

We consider here that we are in the down-quark mass eigenstate basis, and that the λ, λ' couplings have been redefined in terms of the couplings appearing in the superpotential and of the corresponding Cabibbo–Kobayashi–Maskawa matrix elements; however, for simplicity we do not introduce additional notation.

In this model, in order to simplify, we drop the slepton-flavour dependence from $\frac{X}{M_2^{(p)\,2}} f(x_\ell^{(p)})$ and $\frac{X}{M_{q2}^{(p)\,2}} f(x_q^{(p)})$ and consider them to be universal in the slepton and squark sector respectively. We are then led to

$$(m_{qm})_{\text{loop}} = \frac{1}{16\pi^2} X \left(\frac{f(x_\ell)}{M_2^2} \sum_{k,p} \lambda_{qkp} \lambda_{mpk} m_\ell^{(k)} m_\ell^{(p)} + 3\frac{f(x_q)}{M_{q2}^2} \sum_{k,p} \lambda'_{qkp} \lambda'_{mpk} m_q^{(k)} m_q^{(p)} \right). \quad (11)$$

We use the following parametrization for the one-loop mass matrix written in the same basis as the tree-level mass matrix:

$$\mathcal{M}_\nu^{\text{loop}} = \begin{pmatrix} m_{11} & m_{12} & m_{13} \\ m_{12} & m_{22} & m_{23} \\ m_{13} & m_{23} & m_{33} \end{pmatrix}. \quad (12)$$

The loop mass matrix elements m_{ij} are given in appendix C, where we have kept only the relevant contributions after employing the mass hierarchy selection from the charged-lepton and down-quark sector.

Finally, the total mass matrix we consider is

$$\mathcal{M}_\nu = \mathcal{M}_\nu^{\text{tree}} + \mathcal{M}_\nu^{\text{loop}}. \quad (13)$$

An important remark is that there are additional loop corrections that can generate neutrino masses through the sneutrino mass splitting in these models [5]. An additional gaugino–sneutrino (Higgs) loop appears where the R-parity violation is now contained in the mass-mixing term between the sneutrino and antisneutrino. Naively, it can be shown that this effect is small when the soft mass vector $B = B_{\mu_\alpha}$ and the vacuum expectation value vector of the down-type scalar fields v_α are aligned [62,63]. However, a full treatment of this effect requires a one-loop calculation of the scalar mass matrices (Higgses and sleptons), which is beyond the scope of this paper.

A. Toy model

In order to have an idea of how to constrain the whole space of parameters given by the different λ and λ' involved in the loop contribution to the mass and the $\mu_{e,\mu,\tau}$ appearing in

---

[5]We especially thank S. Davidson for discussions on this point.
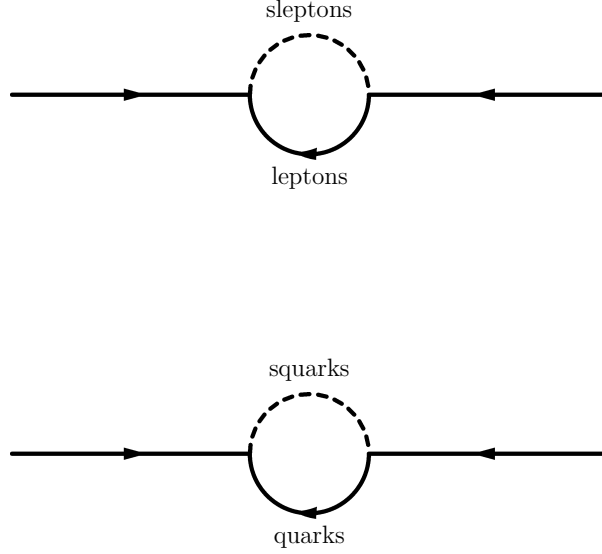
sleptons

leptons

squarks

quarks

FIG. 1. *One-loop Feynman diagrams contributing to the neutrino masses.*

the tree-level mass with the neutrino data, we put ourselves in the naive picture where all the λ couplings are equal and also the λ' couplings. In fact we are naively assuming in eq. (11) (see appendix C) that $\lambda_{133} = \lambda_{233} = \lambda_{333}$ and $\lambda'_{133} = \lambda'_{233} = \lambda'_{333}$.

We thus have two universal trilinear R-parity couplings, λ and λ', and three bilinear couplings, μ_e, μ_μ and μ_τ. In this toy model, our mass matrix can be written as follows

$$\mathcal{M}_\nu = \begin{pmatrix} K_1 + K_2 + \alpha_e^2 & K_1 + K_2 + \alpha_e\alpha_\mu & K_2 + \alpha_e\alpha_\tau \\ K_1 + K_2 + \alpha_e\alpha_\mu & K_1 + K_2 + \alpha_\mu^2 & K_2 + \alpha_\mu\alpha_\tau \\ K_2 + \alpha_e\alpha_\tau & K_2 + \alpha_\mu\alpha_\tau & K_2 + \alpha_\tau^2 \end{pmatrix}, \tag{14}$$

where

$$K_1 = \frac{X}{16\pi^2} \frac{f(x_\ell)}{M_2^2} \left(\lambda^2 m_\tau^2 \right) \;,$$

$$K_2 = 3 \frac{X}{16\pi^2} \frac{f(x_q)}{M_2^{q2}} \left(\lambda'^2 m_b^2 \right) \;. \tag{15}$$

Generically this matrix has three non-zero eigenmasses. Under several different approximations (i.e. $K_1 = 0$, or $K_2 = 0$, or $\alpha_\mu = \alpha_e$), this mass matrix yields only *two* non-zero eigenvalues

$$U^t \times \mathcal{M} \times U = \text{diag}\{0, m_2, m_3\}. \tag{16}$$

The different physical motivations (or limits) for these approximations correspond to the cases where:

- $\lambda = 0$ or $f(x_\ell) = f(x_q)$ and $M_2 = M_2^q$ gives $K_1 = 0$ due to the hierarchy $m_b \gg m_\tau$.

- $\lambda' = 0$ or, if we take the limit in which the squarks decouple, $K_2 = 0$.

10

- assume some hierarchy between the bilinear terms in the Lagrangian, such that $\alpha_e \sim \alpha_\mu \ll \alpha_\tau$.
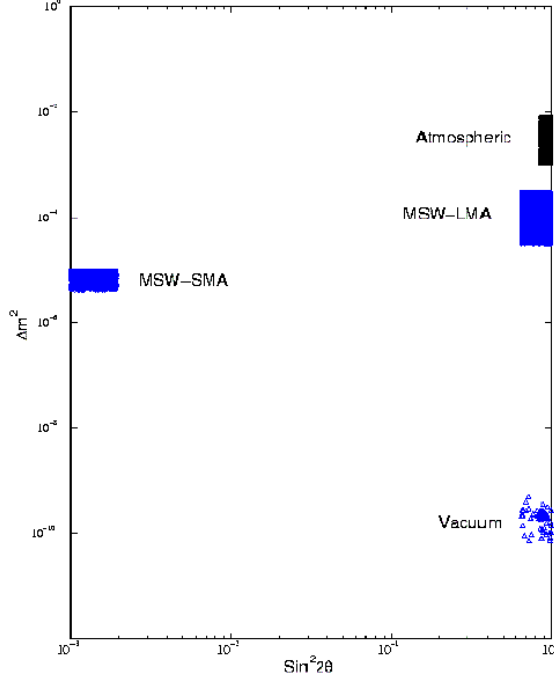
V. RESULTS

A. General results

FIG. 2. Δm^2 in units of eV^2 as a function of $\sin^2 2\theta$. The atmospheric and different solar solutions that are presented result from a combined fit with CHOOZ and SuperK constraints. The atmospheric solution is represented by the parameters $(\Delta m_{13}^2, \sin^2 2\theta_{23})$. The MSW-LMA and MSW-SMA solar solutions are represented by the parameters $(\Delta m_{12}^2$ or Δm_{23}^2 and $\sin^2 2\theta_{12})$ while the vacuum solution is represented by the parameters $(\Delta m_{12}^2, \sin^2 2\theta_{12})$.

We have performed a general scan of parameter space made up by the six matrix elements that appear in eq. (3). In this section we will simply present the results, and our discussion of them is given in the next section. We present in fig. 2 the allowed points on the $(\Delta m^2, \sin^2 2\theta)$ plane, which satisfy the combined constraints (CHOOZ, SuperK and solar data) for the possible solutions of the solar and atmospheric anomalies. Allowing only combined solutions of solar, SuperK and CHOOZ data restricts the available region of parameter space. We also see in fig. 2 that all three possible solutions for the solar anomaly, CHOOZ and atmospheric SuperK bounds can be simultaneously satisfied. After several runs, we choose

11

the interval of variation of the matrix elements M_{ij} in such a way that, combined to CHOOZ, SuperK constraints and one (or all) of the solar solutions is (are) possible. For example, in order to have a combined fit of the vacuum solution for solar anomaly, together with CHOOZ and SuperK constraints then the matrix elements have been varied in the interval -0.5 eV $\leq M_{ij} \leq 0.5$ eV.

We also note that the density of points (solutions) for Vacuum + CHOOZ + SuperK is smaller than the one for MSW-SMA + CHOOZ + SuperK which in turn is much smaller than the one corresponding to MSW-LMA + CHOOZ + SuperK.

Tables III, IV and V, which are given in the next subsections, present the allowed ranges of the input parameters (matrix elements) that satisfy the different solar oscillation solutions together with the CHOOZ *and* the atmospheric SuperK constraints.

To study the spectrum for each of the possible combined solutions we give samples of the different mass spectra for different values of the matrix elements M_{ij}. For illustration, we have present our plots for the spectrum as a function of the matrix element M_{13}, which varies when we scan over parameter space. We also plot the effective mass relevant for neutrinoless double beta decay and the sum of the mass eigenvalues. Our results for the latter two quantities show that for the specific range that we have chosen to satisfy the combined fit of solar, CHOOZ and atmospheric constraints, the present bounds are always satisfied. In fact, for Majorana neutrinos, a slightly stronger bound on the effective mass can be placed by our analysis and will be given below in each subsection. This bound is valid when we vary the mass matrix elements in the ranges that are specified below for each subcase.
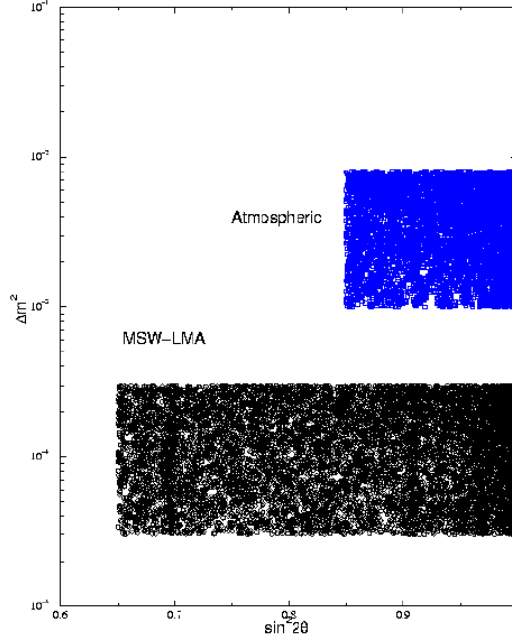
FIG. 3. Δm^2 in units of eV^2 as a function of $\sin^2 2\theta$. The atmospheric and solar solutions that are presented result from a combined fit of MSW-LMA, CHOOZ and SuperK constraints. The atmospheric solutions are represented with the parameters (Δm_{13}^2, $\sin^2 2\theta_{23}$) while the MSW-LMA solar solutions are presented with the parameters (Δm_{12}^2 or Δm_{23}^2 and $\sin^2 2\theta_{12}$).

1. MSW-LMA

For a given model, imposing MSW-LMA, atmospheric SuperK and CHOOZ constraints simultaneously determines the allowed ranges for the input parameters M_{11} (eV), M_{22} (eV), M_{12} (eV), M_{23} (eV), M_{33} (eV), M_{13} in (eV), summarized in table III. In order to obtain these results we have initially allowed all six matrix elements to vary in the interval $[-1.0, +1.0]$ eV.

Figure 3 shows the available regions in parameter space from the combined constraint of SuperK data together with CHOOZ and the MSW-LMA solution.

It is clear from fig. 3 that, with this scan of parameter space, we can cover most of the allowed region that satisfies the combined constraints mentioned above.

In figs. 4a and 4b we plot the results of the individual mass eigenvalues and the effective mass (only valid for Majorana masses) together with the sum of the eigenmasses, which is the relevant quantity for HDM when we impose the constraints simultaneously. We can see from fig. 4a that the hierarchical spectrum is preferred for small values of our parameter M_{13}.

Using the results presented in fig. 4b, for the entire range of variation of the matrix element M_{13}, a strong bound can be placed on the neutrinoless double beta decay effective mass, i.e.
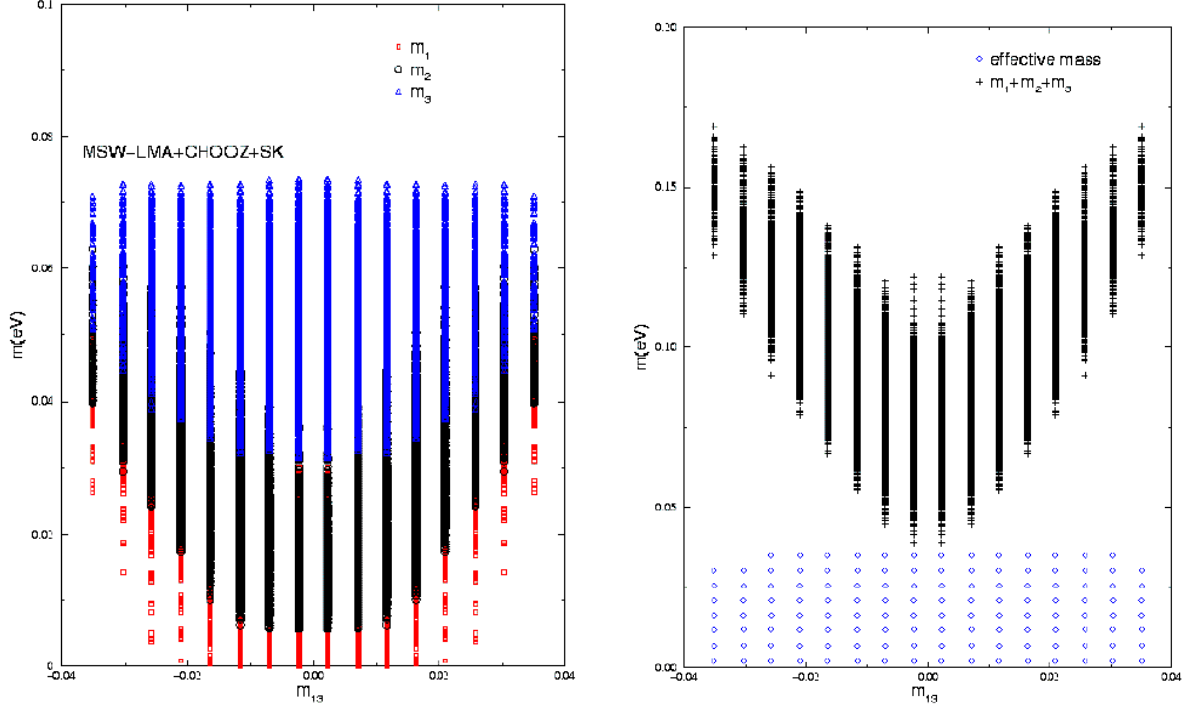
13

(a)　　　　　　　　(b)

FIG. 4. The spectrum presented results from a combined fit with CHOOZ and SuperK and MSW-LMA solar constraints. Mass spectrum (a) which presents the three possible mass eigenvalues (eV). The effective mass and the sum of eigenmasses are given in (b).

for $M_{13} \in [-4, +4] \times 10^{-2}$ eV (while the other matrix elements vary in the intervals given in table III), $m_{\mathrm{eff}} \lesssim 5 \times 10^{-2}$ eV.

2. MSW-SMA

Imposing MSW-SMA, SuperK and CHOOZ constraints simultaneously gives the ranges for the input parameters summarized in table IV. As in the previous section, this illustrative table is valid for a given model in which the mass matrix elements vary initially, before applying the solar, atmospheric and CHOOZ constraints, in the range $[-1.0, +1.0]$ eV.

Figure 5a gives the combined constraint coming from SuperK data together with the CHOOZ bound and the MSW-SMA solution. We have noticed that with our scan of the parameter space the resulting density of points in fig. 5a is much smaller than in the case of MSW-LMA (fig. 3).

We show in fig. 5b the results of the individual mass eigenvalues, the effective mass and the values of Σm_i when we impose the constraints. Here once again there is a bound $m_{\mathrm{eff}} \lesssim few \times 10^{-2}$ eV for $M_{13} \in [-4.0, +4.0] \times 10^{-2}$ eV (the other matrix elements take values in the ranges given in table IV).

14

Inputs	Minimum	Maximum
$M_{11}(10^{-2}\mathrm{eV})$	-2.7	7.3
$M_{12}(10^{-2}\mathrm{eV})$	-4.3	4.3
$M_{13}(10^{-2}\mathrm{eV})$	-3.9	3.9
$M_{22}(10^{-2}\mathrm{eV})$	-1.1	8.3
$M_{23}(10^{-2}\mathrm{eV})$	-7.4	7.4
$M_{33}(10^{-2}\mathrm{eV})$	-5.0	8.9

TABLE III. Allowed ranges of the input parameters that satisfy MSW-LMA, SuperK and CHOOZ constraints simultaneously. They also fulfil neutrinoless double beta decay and cosmological constraints. This illustration is for a model where the allowed inputs vary initially in a given interval, i.e., $M_{ij} \in [-1.0, +1.0]$ eV .

3. Vacuum Solar Solution

In this case, there are few solutions that satisfy simultaneously all of the constraints. One can see in fig. 6a how the allowed points on the $(\Delta m^2, \sin^2 2\theta)$ plane are reduced compared to the density of points in the cases of MSW-LMA (fig. 3) and MSW-SMA (fig. 5a).
The allowed ranges for the input parameters, after imposing the vacuum oscillation solution, SuperK and CHOOZ constraints simultaneously, are summarized in table V. This illustrative table is valid for a given model in which the mass matrix elements vary initially, before applying the solar, atmospheric and CHOOZ constraints, in the range $[-0.5, +0.5]$ eV.
In fig. 6b, where the spectrum of eigenmasses is represented together with the effective mass m_{eff} and the sum over the eigenmasses, a salient feature is the presence of two nearly degenerate eigenvalues ($m_1 \sim m_2$). Here we also have a strong bound on the effective mass $m_{\mathrm{eff}} \lesssim \mathrm{few} 10^{-2}$ eV as we vary M_{13} in $[-4.0, 4.0] \times 10^{-2}$ eV (the other matrix elements take values in the ranges given in table V).

15

Inputs	Minimum	Maximum
$M_{11}(10^{-2}\text{eV})$	-4.0	2.9
$M_{12}(10^{-2}\text{eV})$	-4.0	4.0
$M_{13}(10^{-2}\text{eV})$	-4.0	4.0
$M_{22}(10^{-2}\text{eV})$	-1.3	8.3
$M_{23}(10^{-2}\text{eV})$	-8.0	8.0
$M_{33}(10^{-2}\text{eV})$	-4.0	5.9

TABLE IV. Allowed ranges of the input parameters that satisfy MSW-SMA, SuperK and CHOOZ constraints simultaneously. They also fulfil neutrinoless double beta decay and cosmological constraints. This illustration is for a model where the allowed inputs vary initially in the interval $[-1.0, +1.0]$ eV .
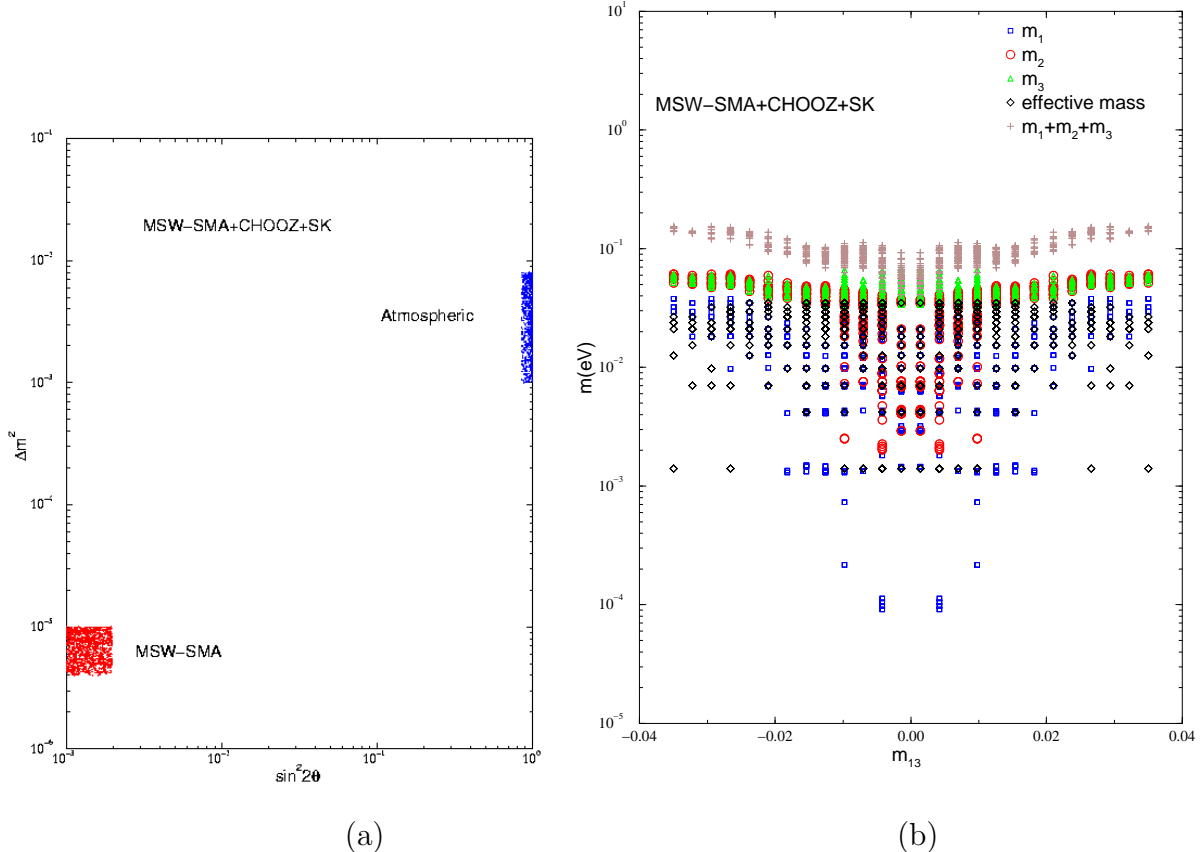

(a)   (b)

FIG. 5. In (a) we represent Δm^2 in units of eV^2 as a function of $\sin^2 2\theta$. The atmospheric solutions are represented with the parameters $(\Delta m_{13}^2, \sin^2 2\theta_{23})$ and the MSW-SMA solar solutions with the parameters $(\Delta m_{12}^2$ or Δm_{23}^2 and $\sin^2 2\theta_{12})$. In (b), the mass spectrum is represented together with m_{eff} and the sum of the eigenvalues (eV). The atmospheric and solar solutions that are presented result from a combined fit with CHOOZ and SuperK constraints.

16
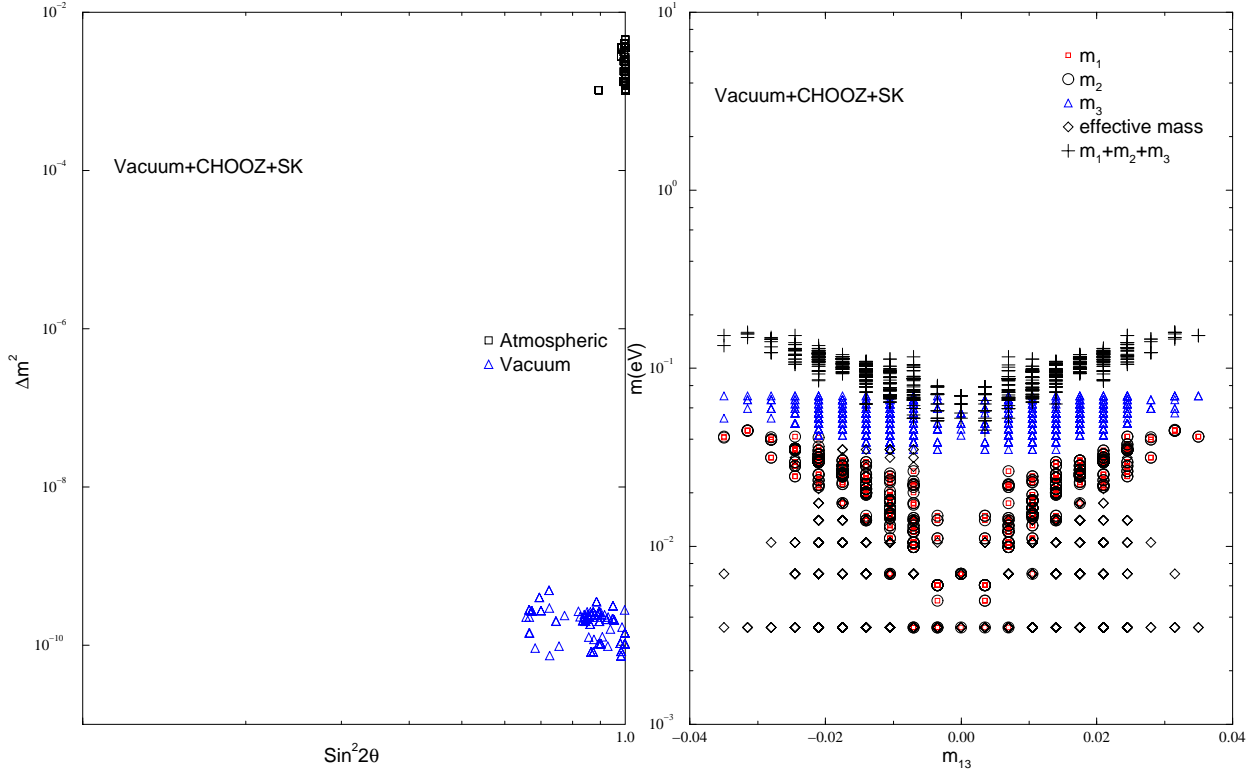
FIG. 6. In (a) we represent Δm^2 in units of eV^2 as function of $\sin^2 2\theta$. The square and the triangle refer to the atmospheric solution (Δm_{13}^2, $\sin^2 2\theta_{23}$) and the vacuum solar solution (Δm_{12}^2, $\sin^2 2\theta_{12}$), respectively. In (b), the mass spectrum is represented together with m_{eff} and the sum of the eigenvalues (eV).

Inputs	Minimum	Maximum
$M_{11}(10^{-2}\text{eV})$	-0.7	1.3
$M_{12}(10^{-2}\text{eV})$	-4.0	4.0
$M_{13}(10^{-2}\text{eV})$	-4.0	4.0
$M_{22}(10^{-2}\text{eV})$	$+0.98$	4.1
$M_{23}(10^{-2}\text{eV})$	-3.5	4.1
$M_{33}(10^{-2}\text{eV})$	$+0.98$	4.1

TABLE V. Allowed ranges of the input parameters that satisfy solar Vacuum, SuperK and CHOOZ constraints simultaneously. They also fulfil neutrinoless double beta decay and cosmological constraints. This illustration is for a model where the allowed inputs vary initially in the interval $[-0.5, +0.5]$ eV .

B. Bounds on R-parity-violating couplings from neutrino data

Our approach to the numerical analysis is to use low energy input without any reference to high-scale physics.

The loop contributions are proportional to different R-parity-violating parameters from those which control the tree-level terms. Three different possibilities can be considered:
- the tree-level contributions are much larger than the loop contributions,
- the tree-level contributions are of the same order as the loop contributions,
- the tree-level contributions are much smaller than the loop contributions.

Applying the results of our general scan of parameter space, we are in fact including all of the above-mentioned cases in our analysis. As each combination of constraints defines a different allowed range of parameters we will present below the corresponding bounds on R-parity-violating couplings separately for each case.

1. MSW-LMA

Imposing MSW-LMA, SuperK and CHOOZ constraints simultaneously defines the ranges for the input parameters K_1 (eV) (which is proportional to λ^2), K_2 (eV) (which is proportional to λ'^2), α_e (eV$^{1/2}$), α_μ (eV$^{1/2}$), α_τ (eV$^{1/2}$), which we have summarized in table VI.

Inputs	Minimum	Maximum
K_1(eV)	0.0	3.0×10^{-2}
K_2(eV)	0.0	2.7×10^{-2}
α_e (eV$^{1/2}$)	-0.114	0.154
α_μ (eV$^{1/2}$)	-0.280	0.28
α_τ (eV$^{1/2}$)	-0.238	0.238

TABLE VI. Allowed ranges of input parameters that satisfy MSW-LMA, SuperK and CHOOZ constraints simultaneously. They also fulfil neutrinoless beta decay and cosmological constraints.

Figure 7 shows the regions that satisfy the combined constraint coming from SuperK data together with CHOOZ and the MSW-LMA solution.

We plot in fig. 8a the results of the individual mass eigenvalues, and in fig. 8b, the effective mass m_{eff} together with the sum over the eigenmasses when we impose all the constraints simultaneously. For illustration, we show how the mass spectrum and the effective mass vary as a function of $x = |\alpha_e(\text{eV}^{1/2})|$. One can read from fig. 8b that in the range of parameters $x \in [0, 0.1]$, we can put a strong bound on the effective mass, that is
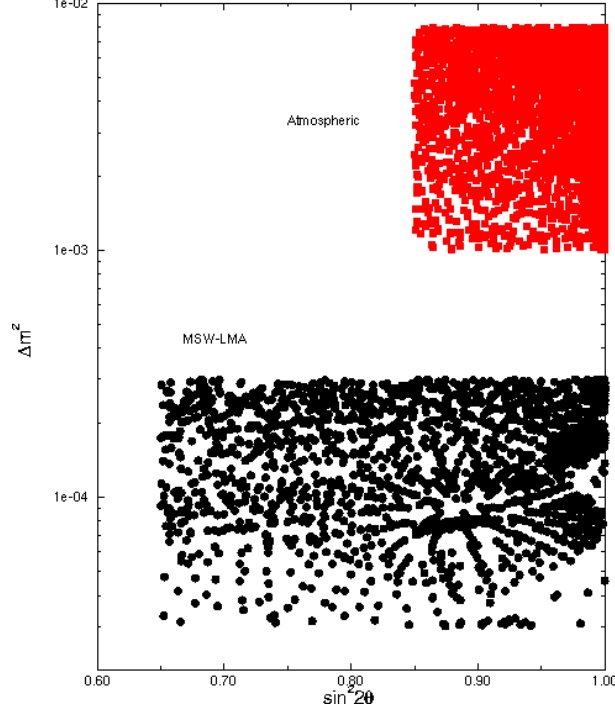
FIG. 7. Δm^2 in units of eV^2 as a function of $\sin^2 2\theta$. The square and the circle refer to the atmospheric solution (Δm_{13}^2, $\sin^2 2\theta_{23}$) and to the MSW-LMA solar solution (Δm_{12}^2, $\sin^2 2\theta_{12}$), respectively.

$m_{\text{eff}} \lesssim 5 \times 10^{-2}$ eV. We can also determine, in the same region of the parameter space, a strong limit on $m_1 + m_2 + m_3 \lesssim 0.2$ eV.

Applying our results from table VI to the specific mass matrix of eq. (14) we find that the following bounds on the R$_{\text{P}}$-violating parameters exist for each solar solution combined with SuperKamiokande and CHOOZ data constraints. For the trilinear couplings we have

$$\lambda^2 \leq \frac{16\pi^2 M_2^2}{X f(x_l) m_\tau^2} \times \left(\mathbf{3.0 \times 10^{-2}} \right), \tag{17}$$

$$\lambda'^2 \leq \frac{16\pi^2 M_2^{q^2}}{3X f(x_q) m_b^2} \times \left(\mathbf{2.7 \times 10^{-2}} \right). \tag{18}$$

Using the results of the appendix B we can also give a bound on the bilinear couplings,

$$\mu_e^2 \leq \frac{4 \det M}{m_Z^2 \cos^2 \beta (M_1 + \tan^2 \theta_W M_2)} \times \left(\mathbf{0.154 \ eV^{-1/2}} \right)^2, \tag{19}$$

$$\mu_\mu^2 \leq \frac{4 \det M}{m_Z^2 \cos^2 \beta (M_1 + \tan^2 \theta_W M_2)} \times \left(\mathbf{0.28 \ eV^{-1/2}} \right)^2, \tag{20}$$

$$\mu_\tau^2 \leq \frac{4 \det M}{m_Z^2 \cos^2 \beta (M_1 + \tan^2 \theta_W M_2)} \times \left(\mathbf{0.238 \ eV^{-1/2}} \right)^2. \tag{21}$$
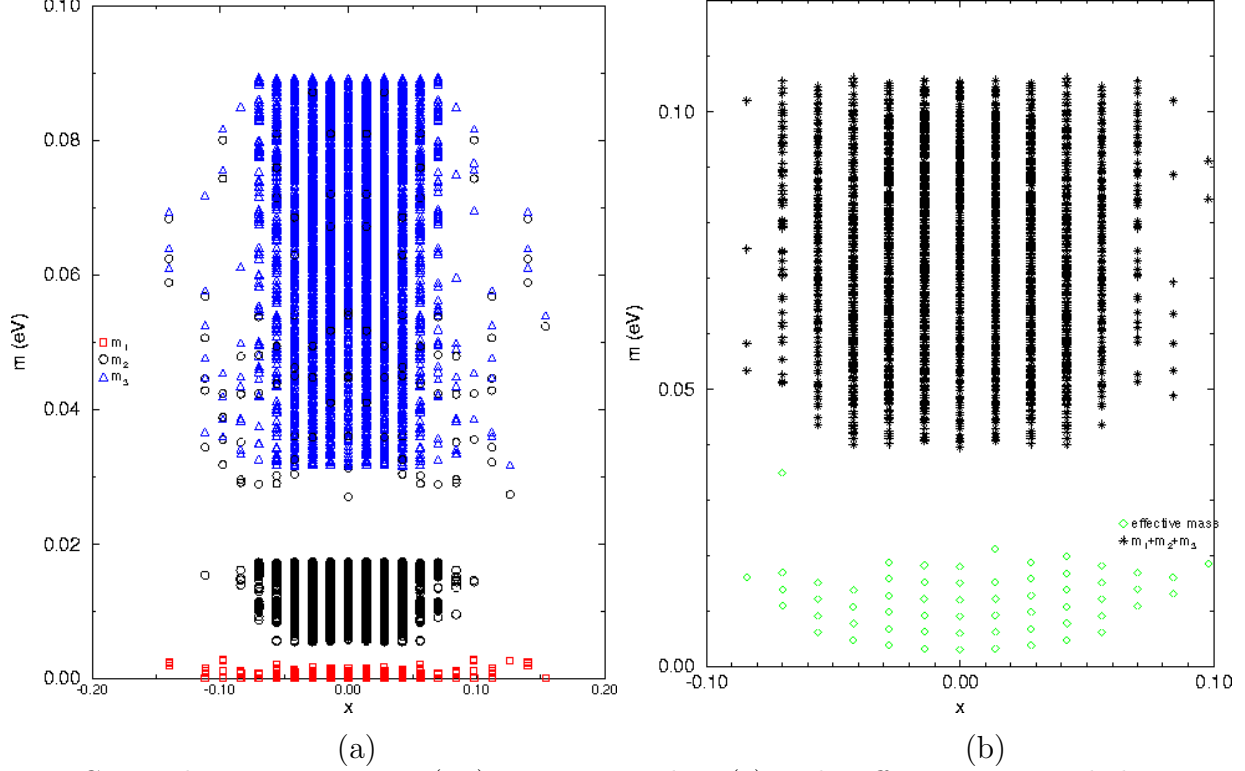
19

FIG. 8. The mass spectrum (eV) is represented in (a). The effective mass and the sum of eigenmasses (eV) are represented in (b). This is when the MSW-LMA solution, the atmospheric one and CHOOZ constraint are imposed simultaneously.

2. MSW-SMA

Imposing MSW-SMA, SuperK and CHOOZ constraints simultaneously determines the ranges for the input parameters given in table VII.

Figure 9 gives the combined constraint coming from SuperK data together with CHOOZ and the MSW-SMA solution. As mentioned previously for our analysis of a generic mass matrix, the density of points is much smaller than in the case of the MSW-LMA solution (fig. 7).

As in the previous subsection by applying our results from table VII to the specific mass matrix of eq. (14) we find the following bounds on the R_P-violating parameters for each solar solution combined with SuperKamiokande and CHOOZ data constraints:

$$\lambda^2 \leq \frac{16\pi^2 M_2^2}{X f(x_l) m_\tau^2} \times \left(\mathbf{3.0 \times 10^{-3}} \right) \;, \tag{22}$$

$$\lambda'^2 \leq \frac{16\pi^2 M_2^{q^2}}{3 X f(x_q) m_b^2} \times \left(\mathbf{3.0 \times 10^{-3}} \right) \;, \tag{23}$$

$$\mu_e^2 \leq \frac{4 \det M}{m_Z^2 \cos^2 \beta (M_1 + \tan^2 \theta_W M_2)} \times \left(\mathbf{4.2 \times 10^{-2} \ eV^{-1/2}} \right)^2 \;, \tag{24}$$

Inputs	Minimum	Maximum
K_1(eV)	0.0	3.0×10^{-3}
K_2(eV)	0.0	3.0×10^{-3}
α_e (eV$^{1/2}$)	-4.2×10^{-2}	4.2×10^{-2}
α_μ (eV$^{1/2}$)	-0.28	0.28
α_τ (eV$^{1/2}$)	-0.21	0.21

TABLE VII. Allowed ranges of the input parameters that satisfy MSW-SMA, SuperK and CHOOZ constraints simultaneously. They also fulfil neutrinoless beta decay and cosmological constraints.

$$\mu_\mu^2 \leq \frac{4 \det M}{m_Z^2 \cos^2 \beta (M_1 + \tan^2 \theta_W M_2)} \times \left(\mathbf{0.28} \ \mathrm{eV}^{-1/2} \right)^2 \ , \tag{25}$$

$$\mu_\tau^2 \leq \frac{4 \det M}{m_Z^2 \cos^2 \beta (M_1 + \tan^2 \theta_W M_2)} \times \left(\mathbf{0.21} \ \mathrm{eV}^{-1/2} \right)^2 \ . \tag{26}$$
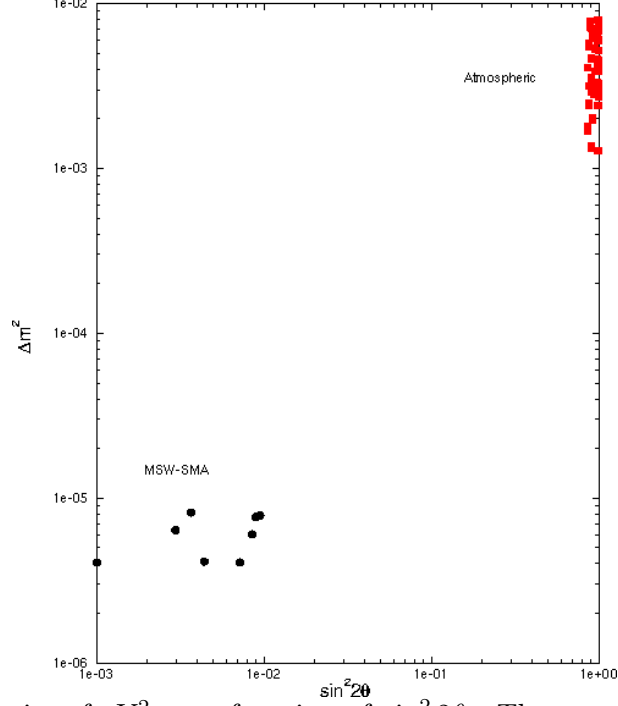
FIG. 9. Δm^2 in units of eV^2 as a function of $\sin^2 2\theta$. The square and the circle refer to the atmospheric solution (Δm_{13}^2, $\sin^2 2\theta_{23}$) and the MSW-SMA solar solution (Δm_{12}^2, $\sin^2 2\theta_{12}$), respectively.

3. Vacuum

In our present application, we find that imposing vacuum oscillations, atmospheric and CHOOZ constraints simultaneously or vacuum oscillation and CHOOZ constraints simultaneously offers no solution of the solar and atmospheric anomalies. We have determined which are the allowed ranges for the input parameters by imposing only vacuum solution constraints; these are summarized in table VIII.

Inputs	Minimum	Maximum
K_1(eV)	0.0	6.0×10^{-3}
K_2(eV)	0.0	1.20×10^{-2}
α_e (eV$^{1/2}$)	-0.35	0.35
α_μ (eV$^{1/2}$)	-0.35	0.35
α_τ (eV$^{1/2}$)	-0.35	0.35

TABLE VIII. Allowed ranges for input parameters that satisfy Vacuum oscillation constraints. They also fulfil neutrinoless beta decay and cosmological constraints.

We determine the bounds on the R_P-violating parameters from the results from table

22

VIII. These are

$$\lambda^2 \leq \frac{16\pi^2 M_2^2}{Xf(x_l)m_\tau^2} \times \left(\mathbf{6.0 \times 10^{-3}}\right) \tag{27}$$

$$\lambda'^2 \leq \frac{16\pi^2 M_2^{q^2}}{3Xf(x_q)m_b^2} \times \left(\mathbf{1.20 \times 10^{-2}}\right) \tag{28}$$

$$\mu_i^2 \leq \frac{4\det M}{m_Z^2 \cos^2\beta(M_1 + \tan^2\theta_W M_2)} \times \left(\mathbf{0.35}\ \mathrm{eV}^{-1/2}\right)^2, \quad i = e, \mu, \tau\ . \tag{29}$$

Given our results for the bounds on the R_P-violating couplings, the analysis in terms of R_P-conserving SUSY parameters is straightforward. Our general results can be analysed by considering the SUSY particle spectrum in detail; we will present these results in a forthcoming paper [64]. A common assumption used to place bounds in this model is to take all R_P-conserving mass parameters to be of the same order, M_{susy}. For the particular case where $M_{susy} = 100$ GeV, $f(x) \to 1$ and $\tan \beta = 2$, the bounds are

- MSW-LMA + CHOOZ + SuperK

$$\lambda^2 \le 1.5 \times 10^{-7} \ , \qquad \lambda'^2 \le 7.02 \times 10^{-9} \ ,$$

$$\mu_e \le 1.9 \times 10^{-4} \text{ GeV}, \quad \mu_\mu \le 3.4 \times 10^{-4} \text{ GeV}, \quad \mu_\tau \le 2.9 \times 10^{-4} \text{ GeV} . \qquad (30)$$

- MSW-SMA + CHOOZ + SuperK

$$\lambda^2 \le 1.5 \times 10^{-8} \ , \qquad \lambda'^2 \le 7.8 \times 10^{-10} \ ,$$

$$\mu_e \le 5.2 \times 10^{-5} \text{ GeV}, \quad \mu_\mu \le 3.4 \times 10^{-4} \text{ GeV}, \quad \mu_\tau \le 2.6 \times 10^{-4} \text{ GeV} . \qquad (31)$$

- Vacuum

$$\lambda^2 \le 3.0 \times 10^{-8} \ , \qquad \lambda'^2 \le 3.1 \times 10^{-9} \ ,$$

$$\mu_i \le 4.3 \times 10^{-4} \text{ GeV}, \quad i = e, \mu, \tau . \qquad (32)$$

C. Dependence of the $(\Delta m^2, \sin^2 2\theta)$ solar and atmospheric parameters on the R_P-violating parameters

We now plot in figs. 10, 11 and 12, the different solar and atmospheric parameters as functions of the R_P-violating parameters $K_1 \propto \lambda^2$, $K_2 \propto \lambda'^2$, $\alpha_{e,\mu,\tau}$ and also $\alpha^2 = \alpha_e^2 + \alpha_\mu^2 + \alpha_\tau^2$.

In figs. 10 and 11, where the constraints from CHOOZ, SuperK and the MSW-LMA solution are satisfied simultaneously, we have plotted the solar parameters Δm_{12}^2 and $\sin^2 2\theta_{12}$ (fig. 10) and the atmospheric variables Δm_{13}^2 and $\sin^2 2\theta_{23}$ (fig. 11). Figure 12 illustrates the dependence of the solar and atmospheric parameters on the sum of the squares of the R_P-violating bilinear terms for the combined fits of SuperK, CHOOZ and MSW-LMA (figs. 12a and 12c) as well as for Super, CHOOZ and MSW-SMA (figs. 12b and 12d). Here one can observe how the region of parameter space from the fit that satisfies MSW-LMA, CHOOZ and SuperK simultaneously is considerably larger than the available region where we fit the MSW-SMA, CHOOZ and SuperK atmospheric constraints.

VI. DISCUSSIONS AND CONCLUSIONS

Our results from the general analysis show that there are many regions in parameter space that can accommodate simultaneously the MSW-LMA and atmospheric oscillation solutions together with the CHOOZ constraint, see figs. 2 and 3. In comparison, we see from fig. 5a that not all of the allowed region in the $(\Delta m^2, \sin^2 2\theta)$ plane is covered when MSW-SMA and the atmospheric oscillations solutions together with the CHOOZ constraints are imposed. Moreover, the region of parameter space for which the atmospheric, CHOOZ and vacuum oscillation constraints are satisfied has very few solutions. In contrast, we find that for the specific case of the MSSM with R-parity violation there are no regions in parameter which can accommodate simultaneously the vacuum solar solution and all other constraints.

As far as the possible spectra are concerned, we clearly see that for the combined MSW-SMA, CHOOZ and SuperK constraints both the hierarchical and pseudo-Dirac spectra are more commonly present. There are also a few values of parameter space that present a degenerate spectrum. For a combination of MSW-LMA, CHOOZ and SuperK constraints, the three possible spectra are very common. As expected, for the combined vacuum oscillation solution, CHOOZ and SuperK constraints only pseudo-Dirac spectra are present. In reference to figs. 4, 5b and 6b our conclusions hold and the bounds mentioned in the previous section are still maintained when we study the spectrum in terms of the other parameters $M_{ij} \neq M_{11}$.

It is clear that increasing the range of variation of our parameters changes the values of the eigenvalues of the mass matrix. In fact, larger values of the inputs make it impossible to satisfy the vacuum oscillation constraints; eventually the same will occur with the MSW-SMA and MSW-LMA solutions. It is really the combination of constraints that solve both atmospheric and solar anomalies which limit the allowed ranges. An important conclusion is that, after obtaining a simultaneous solution for the solar and atmospheric anomalies and the CHOOZ constraint, the effective mass constraint and the cosmological constraint are always satisfied. We have also indicated previously when a stronger bound can be placed on these quantities.

Some of the previous work regarding neutrino masses in this specific model we consider have tried to fit only one of the Δm^2 to either the atmospheric or one of the solar solutions. From our analysis we have seen that fitting only one of the neutrino anomalies is straightforward. What is much harder to obtain is a region in parameter space that satisfy the combined fits. Other authors have also studied the possibility of fitting both atmospheric and solar anomalies, although their approaches are somewhat different from ours. They consider either supergravity-inspired models or exclusively bilinear contributions, or exclusively

trilinear contributions.

The usual bounds [65,66] cited for the trilinear couplings λ_{133} and λ'_{133} are placed when only one of these two R-parity-violating couplings are considered to be present in the theory. The bound is implemented by using the upper bound on the electron neutrino mass from the ^{3}H β-decay spectrum. Having only one of the trilinears corresponds of course to having a single non-zero matrix element in eq. (14), given by K_1 or K_2 depending on whether the trilinear coupling is λ_{133} or λ'_{133}, respectively. We see that in the special limits we have considered on R-parity-conserving SUSY parameters our bounds from eq. (30) agree with the previous bounds. The overall conclusion is that the bounds are very strong on the R-parity violating parameters. We have shown that the simultaneous inclusion of many of these couplings can constrain them much more than other bounds arising from other low-energy or high-energy processes [65,66]. The overall conclusion is that the bounds are very strong on the R-parity violating parameters.

Figures 10-12 illustrate the different dependences of the solar and atmospheric parameters on the R-parity couplings. It is clear that for large values of the parameters there are no solutions. The discreteness of the allowed values of the parameters is due in part to the step we use in our scan of the parameter space. We also see, of course, that the dependence on a single parameter is complicated, since many solutions can be found for the same value of the variable. This is due to the large number of different parameters involved.

The general global interpretation of the experimental data is that the SuperK seriously challenges MSW-SMA and Vacuum Oscillations solutions [67]. This is in agreement with the analysis we have done. Indeed, the majority of the solar anomaly solutions we have that also satisfy both SuperK and CHOOZ are MSW-LMA. The future experiments SNO, BOREXINO, ICARUS, HERON with solar neutrinos as well as KAMLAND, K2K, MINOS, BooNE..., and many others, will provide additional decisive information to pin down the neutrino mysteries.
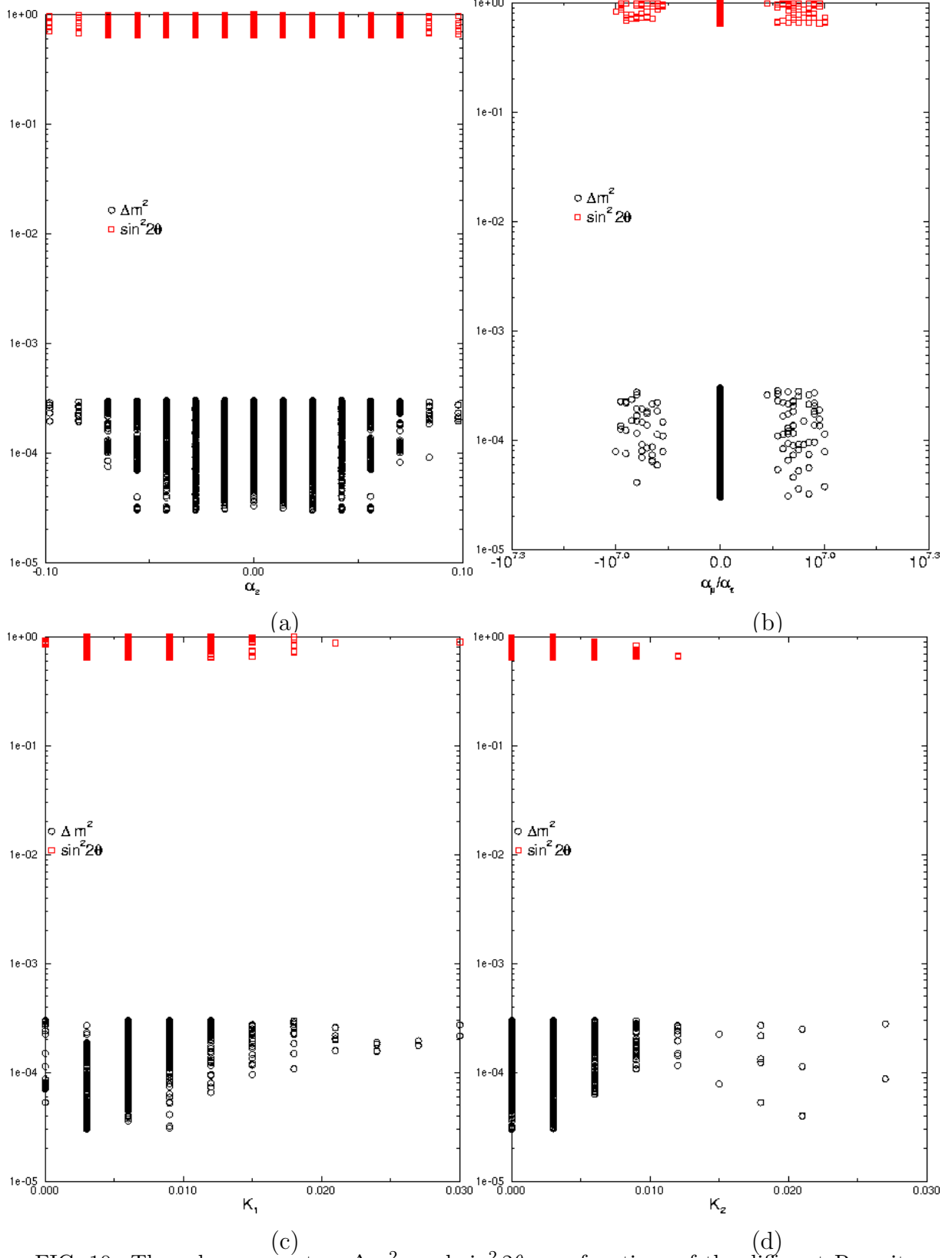
FIG. 10. The solar parameters Δm_{12}^2 and $\sin^2 2\theta_{12}$ as functions of the different R-parity parameters α_e (a), α_μ/α_τ (b), K_1 ($\propto \lambda^2$) (c) and K_2 ($\propto \lambda'^2$) (d), in the case of a combined fit with MSW-LMA, SuperK and CHOOZ constraints.

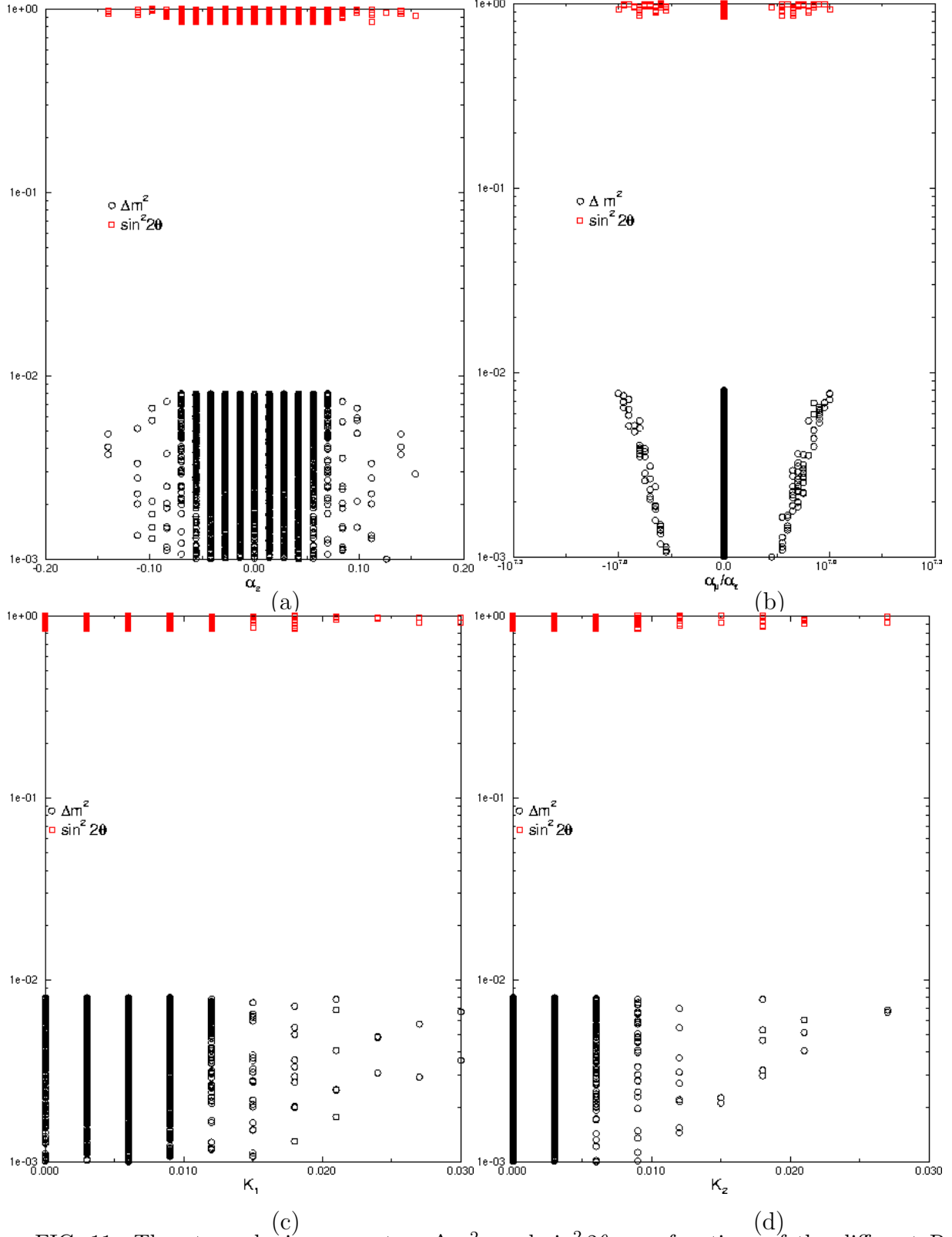FIG. 11. The atmospheric parameters Δm^2_{13} and $\sin^2 2\theta_{23}$ as functions of the different $\mathrm{R_P}$ parameters α_e (a), α_μ/α_τ (b), K_1 ($\propto \lambda^2$) (c) and K_2 ($\propto \lambda'^2$) (d), in the case of a combined fit with MSW-LMA, SuperK and CHOOZ constraints.
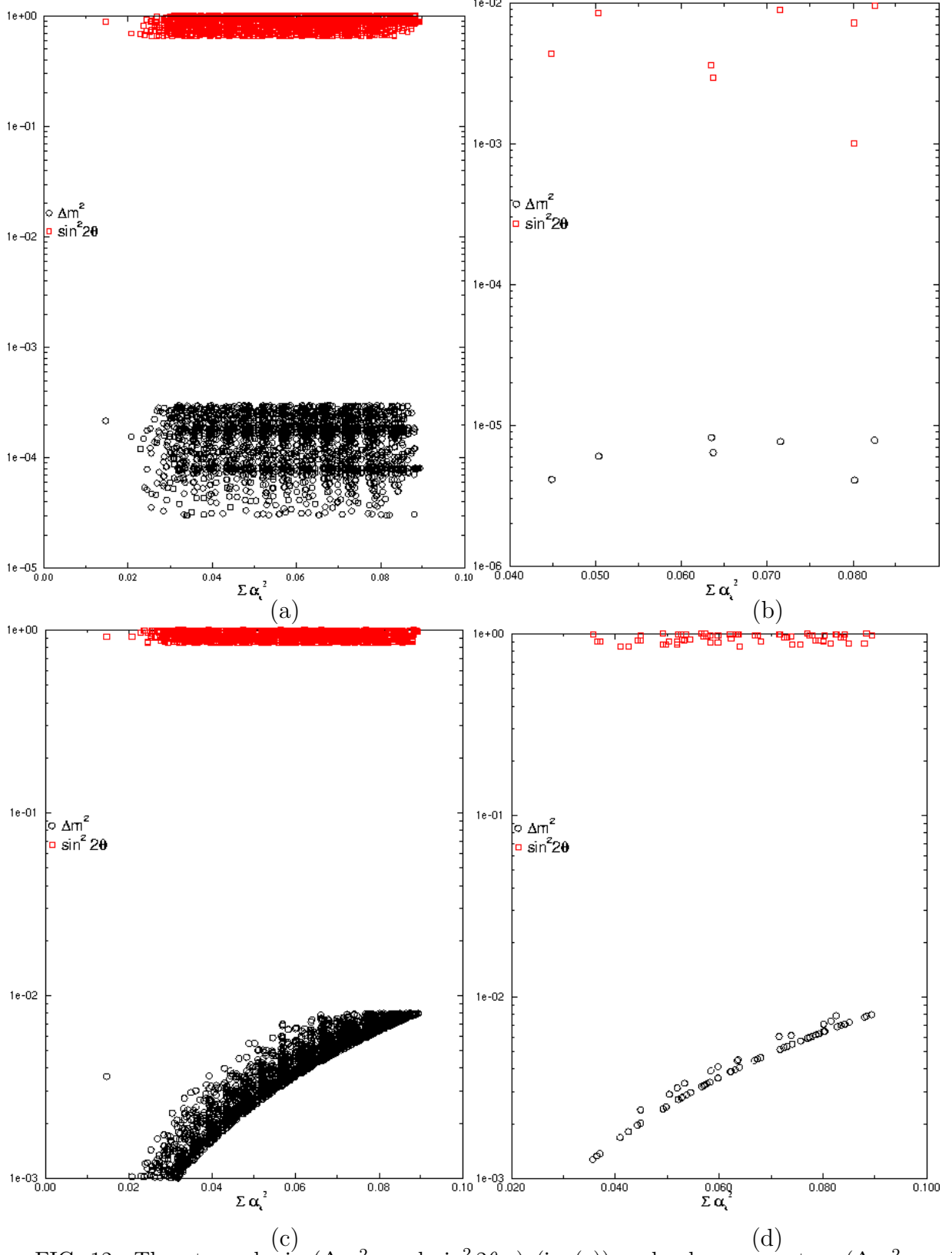
FIG. 12. The atmospheric (Δm_{13}^2 and $\sin^2 2\theta_{23}$) (in (a)) and solar parameters (Δm_{12}^2 and $\sin^2 2\theta_{12}$) (in (c)) as functions of $\alpha^2 = \alpha_e^2 + \alpha_\mu^2 + \alpha_\tau^2$ in the case of MSW-LMA solution (a) and (c) and in the case of MSW-SMA (b) and (d). SuperK and CHOOZ constraints are also imposed.

Charged and Neutral Fermion Mass Matrices

APPENDIX A: CHARGED COLOUR-SINGLET MASS MATRIX

Written in the basis $\Psi = (-i\lambda_-, \psi_{L_o}^2, \psi_{L_1}^2, \psi_{L_2}^2, \psi_{L_3}^2)$, the matrix

$$\mathcal{M}_c^{tree} = \begin{pmatrix} M_2 & \frac{g_2 v \sin\beta}{\sqrt{2}} & 0 & 0 & 0 \\ \frac{g_2 v \cos\beta}{\sqrt{2}} & \mu_o & 0 & 0 & 0 \\ 0 & \mu_1 & m_1 & 0 & 0 \\ 0 & \mu_2 & 0 & m_2 & 0 \\ 0 & \mu_3 & 0 & 0 & m_3 \end{pmatrix} , \tag{A1}$$

can be diagonalized explicitly to obtain the charginos and charged-lepton tree-level masses. However, our analysis of the neutrino spectrum requires the μ_i's to be very small, thus their effect on the eigenvalues and corresponding mass eigenstates will be tiny. It is a good approximation for small R-parity violation to neglect the RPV contribution to the masses in the charged leptons and charginos [68].

APPENDIX B: TREE-LEVEL NEUTRAL COLOUR-SINGLET MASS MATRIX

$$\mathcal{M}_N^{\text{tree}} = \begin{pmatrix} M & \xi^T \\ \xi & m_\nu^o \end{pmatrix} = \begin{pmatrix} M_1 & 0 & \frac{g_1 v \sin\beta}{\sqrt{2}} & -\frac{g_1 v \cos\beta}{\sqrt{2}} & 0 & 0 & 0 \\ 0 & M_2 & \frac{g_2 v \sin\beta}{\sqrt{2}} & -\frac{g_2 v \cos\beta}{\sqrt{2}} & 0 & 0 & 0 \\ \frac{g_1 v \sin\beta}{\sqrt{2}} & -\frac{g_2 v \sin\beta}{\sqrt{2}} & 0 & \mu_o & -\mu_1 & -\mu_2 & -\mu_3 \\ -\frac{g_1 v \cos\beta}{\sqrt{2}} & \frac{g_1 v \sin\beta}{\sqrt{2}} & -\mu_o & 0 & 0 & 0 & 0 \\ 0 & 0 & -\mu_1 & 0 & 0 & 0 & 0 \\ 0 & 0 & -\mu_2 & 0 & 0 & 0 & 0 \\ 0 & 0 & -\mu_3 & 0 & 0 & 0 & 0 \end{pmatrix} , \tag{B1}$$

In the limit where the μ_i's are small, the effective neutrino mass matrix has the "see-saw" structure

$$\mathcal{M}_\nu^{\text{tree}} = -\xi M^{-1}\xi^T + m_\nu^o . \tag{B2}$$

The assumption we make so as to include the one-loop corrections is that only the corrections to m_ν^o need be considered, thus giving the one-loop-corrected expression for the 3×3 neutrino mass matrix [42], [50], [58]:

$$\mathcal{M}_\nu = -\xi M^{-1}\xi^T + \mathcal{M}_\nu^{\text{loop}} , \tag{B3}$$

where $\mathcal{M}_\nu^{\text{loop}} = m_\nu^o + m_\nu^{\text{loop}}$. The expression for m_ν^{loop} is given in the next subsection. The elements of the matrix $M_\nu^{\text{tree}} = \xi M^{-1} \xi^T$, which is parametrized in terms of the α_i's of eq. (6) are given by

$$M_{\nu_{ij}}^{\text{tree}} = g_2^2 \frac{(M_1 + \tan^2 \theta_W M_2)}{4 \det M} \mu_i \mu_j v_1^2, \tag{B4}$$

as we are working in the basis where the slepton vacuum expectation value is zero, $v_1 = v_d = v \cos \beta$. The basis-invariant expression corresponds to substituting $\mu_i \mu_j v_1^2$ with $(\mu < v_i > -\mu_i v_1)(\mu \langle v_j \rangle - \mu_j v_1)$, where $\langle v_i \rangle$ is the vacuum expectation value of the slepton fields L_i[6].

APPENDIX C: LOOP-MASS MATRIX

Expliciting the indices in eq. (7) leads to the following symmetric matrix elements of which we keep only the relevant contributions due to the mass hierarchy in the charged-lepton sector $m_e \ll m_\mu \ll m_\tau$ and in the down-quark sector $m_d \ll m_s \ll m_b$:

$$m_{11}^{\text{loop}} = \frac{X}{16\pi^2} \left(\frac{f(x_\ell)}{M_2^2} \left(\lambda_{133}'^2 m_\tau^2 \right) + 3 \frac{f(x_q)}{M_2^{q2}} \left(\lambda_{133}'^2 m_b^2 + \lambda_{123}' \lambda_{132}' m_s m_b \right) \right) \tag{C1}$$

$$m_{12}^{\text{loop}} = \frac{X}{16\pi^2} \left(\frac{f(x_\ell)}{M_2^2} \left(\lambda_{133} \lambda_{233} m_\tau^2 \right) + 3 \frac{f(x_q)}{M_2^{q2}} \left(\lambda_{133}' \lambda_{233}' m_b^2 + (\lambda_{132}' \lambda_{223}' + \lambda_{123}' \lambda_{232}') m_s m_b \right) \right) \tag{C2}$$

$$m_{13}^{\text{loop}} = \frac{3 \, X}{16\pi^2} \frac{f(x_q)}{M_2^{q2}} \, \lambda_{133}' \lambda_{333}' m_b^2 \tag{C3}$$

$$m_{22}^{\text{loop}} = \frac{X}{16\pi^2} \left(\frac{f(x_\ell)}{M_2^2} \left(\lambda_{233}^2 m_\tau^2 \right) + 3 \frac{f(x_q)}{M_2^{q2}} \left(\lambda_{233}'^2 m_b^2 + \lambda_{223}' \lambda_{232}' m_s m_b \right) \right) \tag{C4}$$

$$m_{23}^{\text{loop}} = \frac{3 \, X}{16\pi^2} \frac{f(x_q)}{M_2^{q2}} \, \lambda_{233}' \lambda_{333}' m_b^2 \tag{C5}$$

$$m_{33}^{\text{loop}} = \frac{3 \, X}{16\pi^2} \frac{f(x_q)}{M_2^{q2}} \, \lambda_{333}'^2 m_b^2 \tag{C6}$$

---

[6]For a general discussion of basis-independent parametrizations of R-parity violation, see refs. [69].

REFERENCES

[1] Y. Fukuda et al., Super-Kamiokande Collaboration, Phys. Lett. **B 433** (1998) 9; Phys. Lett. **B 436** (1998) 33; Phys.Rev.Lett. **81** (1998) 1562.

[2] R. Becker-Szendy et al., IMB Collaboration, Nucl. Phys. **B** (Proc. Suppl.) **38** (1995) 331.

[3] W.W.M. Allison et al. Soudan-2 Collaboration, Phys. Lett. **B391** (1997) 491, Phys. Lett. **B449** (1999) 137.

[4] Y. Fukuda et al., Kamiokande Collaboration, Phys. Lett. **B 335** (1994) 237.

[5] R. Davis et al., Phys.Rev.Lett. **21** (1968) 1205; B.T. Cleveland et al., Astrophys. J. **496** (1998) 505.

[6] W. Hampel et al., Phys. Lett. **B 388** (1996) 384.

[7] D.N. Abdurashitov et al., Phys. Rev. Lett. **B 77** (1996) 4708; astro-ph/9907131.

[8] K. S. Hirata et al., Kamiokande Collaboration, Phys. Rev. Lett. **77** (1996) 1683.

[9] Y. Fukuda et al., Super-Kamiokande Collaboration, Phys.Rev.Lett. **81** (1998) 1158.

[10] M. Ambrosio et al., MACRO Collaboration, Phys. Lett. **B 434** (1998) 451.

[11] C. Anthanassopoulos et al., LSND Collaboration, Phys. Rev. Lett. **B 81** (1998) 1774.

[12] S. Coleman and S.L. Glashow, Phys. Rev. **D59** 116008 and references therin.

[13] A. Halprin and H.B. Kim. KIAS-P99028, preprint hep-ph/9905301 and references therin.

[14] S. Pakvasa, hep-ph/9905426.

[15] G.L. Fogli, E. Lisi, A. Marrone and G. Scioscia, Phys.Rev. **D60** 053006 and Phys.Rev. **D59** 117303.

[16] B. Zeitnitz et al.,KARMEN Collaboration Prog.Part.Nucl.Phys. **40** (1998) 169.

[17] see for example and refs. therein: R.Barbieri, J. Ellis and M.K. Gaillard, Phys. Lett. **B90** (1980) 249; M. Gell-Mann, P. Ramond and R. Slansky, *Proceedings of the Supergravity Stony Brook Workshop*, New York 1979, eds. P. Van Nieuwenhuizen and D. Freedman; T. Yanagida, *Proceedinds of the Workshop on Unified Theories and Baryon Number in the Universe*, Tsukuba, Japan 1979, ed.s A. Sawada and A. Sugamoto; S. Dimopoulos, L.J. Hall and S. Raby, Phys. Rev. Lett. **68** (1992) 1984; G.K. Leontaris et al, Phys. Rev. **D53** (1996) 6381; S. Lola and J. D. Vergados, Prog. Part. Nucl. Phys.**40** (1998) 71; G. Altarelli and F. Feruglio, hep-ph/9905536 and hep-ph/9907532; J.A. Casas et al,

hep-ph/9905381 and hep-ph/9906281; M. Carena et al, hep-ph/9906362; P. Langacker, Nucl. Phys. Proc. Suppl. **77** (1999) 241; Z. Berezhiani and A. Rossi, JHEP **9903** (1999) 002.

[18] R. Barbieri, L.J. Hall, D. Smith, A. Strumia and N. Weiner, JHEP **9812** (1998) 017.

[19] G. Gelmini and E. Roulet, Rept. Prog. Phys. **58** (1995) 1207.

[20] B. Kayser, F. Gibrat-Bebu and F. Perrier, *The Physics of Massive Neutrinos*, Wolrd Scientific, Singapore 1989.

[21] S.M. Bilenkii, C. Giunti, W. Grimus, hep-ph/9812360.

[22] J.W.F. Valle, hep-ph/9809234.

[23] M. Apollonio et al., CHOOZ Collaboration, Phys. lett. **B 420** (1998) 397.

[24] H. Georgi and S.L. Glashow, hep-ph/9808293.

[25] M. Günther et al., Phys. Rev. **D55** (1997) 54, Phys. lett. **B 407** (1997) 219.

[26] L. Baudis et al., Phys. Lett. **B 407** (1997) 219.

[27] R.A.C. Croft, W. Hu and R. Davé, astro-ph/9903335, and see references therein.

[28] V. M. Lobashev, to be published in the proceedings of 17th International Workshop on Weak Interactions and Neutrinos (WIN 99), Cape Town, South Africa, 24-30,Jan 1999; Prog.Part.Nucl.Phys.**40** (1998) 337.

[29] H. Barth, Prog.Part.Nucl.Phys.**40** (1998) 353, J. Bonn, to be published in the proceedings of 17th International Workshop on Weak Interactions and Neutrinos (WIN 99), Cape Town, South Africa, 24-30,Jan 1999.

[30] G. Gelmini, to be published in the proceedings of 17th International Workshop on Weak Interactions and Neutrinos (WIN 99), Cape Town, South Africa, 24-30, Jan 1999, hep-ph/9904369.

[31] G.L. Fogli, E. Lisi, A. Marrone and G. Scioscia, Phys. Rev. **D59** 33001.

[32] V. Barger, T.J. Weiler and K. Whisnat, Phys. Lett. **B440** (1998)1.

[33] M. C. Gonzalez-Garcia, H. Nunokawa, O.L. G. Peres and J.W.F. Valle, Nucl. Phys. **B543** (1999) 3.

[34] J.N. Bahcall, P.I. Krastev and A.Yu. Smirnov, Phys. Rev. **D58** 96016.

[35] N. Hata and P. Langacker, Phys. Rev. **D56** (1997) 6117.

[36] S.T. Petcov, to be published in the proceedings of 17th International Workshop on Weak Interactions and Neutrinos (WIN 99), Cape Town, South Africa, 24-30, Jan 1999, hep-ph/9907216.

[37] L.L. Chau and W.Y. Keung, Phys.Rev.Lett. **53** (1984) 1802.

[38] R. Godbole, P. Roy and X. Tata, Nucl. Phys. **B401** (1993) 67.

[39] Y. Grossman, H.E. Haber Phys.Rev. **D59** 093008.

[40] E.Nardi, Phys. Rev. **D55** (1997) 5772.

[41] T. Banks, Y. Grossman, E. Nardi and Y. Nir, Phys. Rev. **D52** (1995) 5319.

[42] M. Nowakowski and A. Pilaftsis, Nucl. Phys. **B461** (1996) 19.

[43] F.M. Borzumati, Y. Grossman, E. Nardi and Y. Nir, Phys.Lett. **B384** (1996) 123.

[44] R. Hempfling Nucl.Phys. B478 (1996) 3.

[45] B. de Carlos and P. White, Phys. Rev. **D54** (1996) 3427.

[46] A.Y. Smirnov and F. Vissani, Nucl. Phys. **B460** (1996) 37.

[47] H.P. Nilles and N. Polonsky, Nucl. Phys. **B499** (1997) 33.

[48] D.E. Kaplan and A.E. Nelson, hep-ph/9901254.

[49] E.J. Chun and J.S. Lee, hep-ph/9811201.

[50] V. Bednyakov, A. Faessler and S. Kovalenko, Phys. Lett. **B442** (1998) 203.

[51] J.C. Romão, hep-ph/9907466.

[52] S.Y. Choi, E.J. Chun, S.K. Kang and J.S. Lee, hep-ph/9903465.

[53] M. Dress, S. Pakvasa, X. Tata and T. ter Veldhuis, Phys. Rev. **D57** (1997) 5335.

[54] S. Rakshit, G. Bhattacharyya and A. Raychadhuri, Phys. Rev. **D59** 091701.

[55] G. Bhattacharyya, H.V. Klapdor-Kleingrothaus, H. Pas, hep-ph/9907432.

[56] E.J. Chun, S.K. Kang, C.W. Kim and J.S. Lee, Nucl. Phys. **B544** (1999) 89.

[57] K. Choi, E.J. Chun and K. Hwang, hep-ph/9811363.

[58] O.C.W. Kong, Mod. Phys. Lett. **A14** (1999) 903.

[59] A. Joshipura and S. Vempati, hep-ph/9903435. A. Joshipura, V. Ravindran and S. Vempati, Phys. Lett **B451** (1999) 98; A. Joshipura and M. Nowakowshi, Phys. Rev.

D51 (1995) 2421.

[60] A. Datta, B. Mukhopadhyaya and S. Roy, hep-ph/9905549.

[61] H. Haber and G. Kane, Nucl. Phys. **B272** (1986) 1.

[62] S. Davidson and S. King, Phys. Lett. **B445** (1998) 191.

[63] Y. Grossman and H. Haber, Phys. Rev. Lett. **78** (1997) 3438; hep-ph/9906310.

[64] A. Abada and M. Losada, in preparation.

[65] H. Dreiner, hep-ph/9707435.

[66] G. Bhattacharyya, Nucl. Phys. Proc. Suppl. **52A** (1997) 83 and hep-ph/9709395.

[67] Chang Kee Jung, Talk given at International Europhysics Conference on High-Energy Physics (EPS-HEP 99), Tampere, Finland, 15-21 Jul 1999.

[68] M. Bisset, Otto C.W. Kong, C. Macenasu and Lynne Orr, hep-ph/9811498 (1998).

[69] S. Davidson and J. Ellis, Phys. Lett. **B39** (1997) 210; Phys. Rev. **D56** (1997) 4182.